Polymeric Proton Conducting Systems Based on Commercial Elastomers. II. Synthesis and Microstructural Characterization of Films Based on HSBR/EPDM/PP/PS/Silica

P. G. Escribano, A. Nacher, C. Del Rio, L. González, J. L. Acosta

Instituto de Ciencia y Tecnología de Polímeros (CSIC), c/Juan de la Cierva 3, 28006 Madrid, Spain

Received 6 November 2003; accepted 25 March 2004
DOI 10.1002/app.20741
Published online in Wiley InterScience (www.interscience.wiley.com).

ABSTRACT: This article reports on the synthesis and structural characterization of films containing hydrogenated poly(butadiene-styrene) block copolymer/ethylene-propylene terpolymer/polypropylene, hydrogenated poly(butadiene-styrene) block copolymer/ethylene-propylene terpolymer/polystyrene, and hydrogenated poly(butadiene-styrene block copolymer/ethylene-propylene terpolymer/silica) crosslinked with peroxides and heterogeneously sulfonated. Sulfonation of the different polymeric systems gives rise to materials with high proton conductivity and great dimensional stability, suited for application in a variety of electronic devices. © 2004 Wiley Periodicals, Inc. J Appl Polym Sci 93: 2394–2402, 2004

Key words: membranes; crosslinking; mechanical properties; rheology; DSC

INTRODUCTION

Polymeric fuel cells are devices capable of converting the chemical energy initially stored in a fuel (generally hydrogen) into electric energy by means of electrochemical reactions. They are operative at low temperature and their principal application refers to transportation and portable electronic systems.[1,2]

Polymeric membrane has some important functions in a fuel cell: to allow protons to pass across the material (when it is hydrated); to act us barrier between reagents, oxygen, and hydrogen; and to be a electronic insulator between the electrodes. Moreover, membrane must have low price, good mechanical and chemical properties, and dimensional stability and can form films about 100 μm. Nafion, material actually utilized in proton exchange membrane fuel cell (PEMFC), is very resistant to chemical attack and strongly hydrophobic. It is a material with high mechanical and chemical resistance, capable of absorbing lots of water, and protons can move freely in the material, but Nafion presents several inconveniences (i.e., it is very expensive, has high proton conductivity but deficient dimensional stability, and is difficult to eliminate from urban and industrial waste). For the purpose of achieving adequate commercial products, new materials must be synthesized to overcome the inconveniences of Nafion.[3–5]

Correspondence to: P. G. Escribano.

Journal of Applied Polymer Science, Vol. 93, 2394–2402 (2004)

It was the aim of this research to obtain polymeric membranes possessing a high proton conductivity and high chemical and dimensional stability. To this end, composite films were synthesized and characterized based on hydrogenated poly(butadiene-styrene) block copolymer, ethylene-propylene terpolymer, polypropylene, polystyrene, and silica, in different compositions. All the samples were cured and subsequently subjected to heterogeneous sulfonation.

EXPERIMENTAL

The following initial materials were used: hydrogenated poly(butadiene-styrene) block polymer (30/70), 2.6% insaturation (HSBR) Calprene BB13 CH 6110, Repsol (Spain; $T_{g\text{-butadiene}} = -56.12$°C and $T_{g\text{-styrene}} = 95.31$°C); ethylene-propylene terpolymer, 8% ethylene norbornene, and 48% ethylene (EPDM) BUNA G 3850 ($T_g = -51.48$°C); polypropylene (PP) 099 ISPLEN, Repsol ($T_m = 164.97$°C and $T_g = 123.13$°C); polystyrene (PS) Polystyrol 143 E, Basf (Germany; $T_g = 88.52$°C), and silica Ultrasil VN3, Degussa (Germany). PP is a semicrystalline polymer that gives dimensional stability to the blend. PS is a amorphous polymer that supplies more groups able to be sulfonated increasing the conductivity; and silica is a very hygroscopic material and also gives structural stability to the material.

The blends were synthesized in an internal mixer, model Haake Rheomix 600, utilizing roller-type rotors at a blending temperature close to the melting temperature of PP, PS, or silica, depending on the blend,

TABLE I
Blend Compositions from Initial Materials

Sample	HSBR (wt %)	EPDM (wt %)	PP (wt %)	PS (wt %)	Silica (wt %)
BG-01	45	45	10	—	—
BG-02	40	40	20	—	—
BG-11	45	45	—	10	—
BG-12	40	40	—	20	—
BG-21	45	45	—	—	10
BG-22	40	40	—	—	20

and at a rate of 90 rpm. Table I compiles the blend compositions under study.

For blend curing, dicumile peroxide was added as a curing agent in the proportion of 2 g peroxide for every 100 g blend in a roller mixer heated to 50°C, cutting and rolling the material several times to ensure homogeneous dispersion of the curing agent.

The crosslinking process of each blend was studied with a Monsanto rheometer, model Rheometer MDR 2000E, determining the most suitable crosslinking conditions. The rheometric tests were conducted at a temperature of 160°C and for 1 h.

The films from the crosslinked materials were obtained by compression molding on a hydraulic Collins press heated by means of a thermofluid. Material input was 2 g per film compressed for a few minutes at maximum pressure (200 kg/cm^2) between the two metal plates, at a temperature below that of crosslinking so as to ease material flow. Then, the temperature was raised to T_{curing} and held there for a time span equal to t_{97}, also at maximum pressure. Subsequently, the sample was cooled in the press to 75°C prior to extracting the film sample, which presents a mean thickness of 100–120 μm.

The traction properties of all the samples were conducted by using an Instron dynamometer, model 4301, and Halterian type, yet nonstandard samples, thickness 100–120 μm, as obtained from the films prepared in the press with the procedure described above.

Residual compression-induced strain was determined at 100°C for 22 h 30 min standard test time, but only for the crosslinked samples, as this test is not applicable to noncrosslinked and sulfonated samples, due to the risk of material degradation at high pressure and temperature. Prior to placing the samples into the deformation molds, their initial thickness was measured. Then, a pressure equal to 25% of their thickness was applied. Subsequently, they were held at room temperature for 30 min, and their thickness was measured again. The strain undergone is

$$= \frac{e_i - e_f}{e_i - e_{gep}} \times 100 \quad (1)$$

Microhardness of the films was measured with a Bareiss durometer.[6]

Differential scanning calorimetry (DSC) of the samples was implemented with a Mettler TA 4000 instrument. The samples were heated to 220°C (to 300°C in the case of the sulfonated samples) for 5 min, so as to eliminate their thermal antecedents. Subsequently, they were quenched to −200°C to be gradually reheated and then allowed to cool to room temperature.

DSC analysis permits insight into the major thermal transitions of the noncrosslinked, cured, and sulfo-

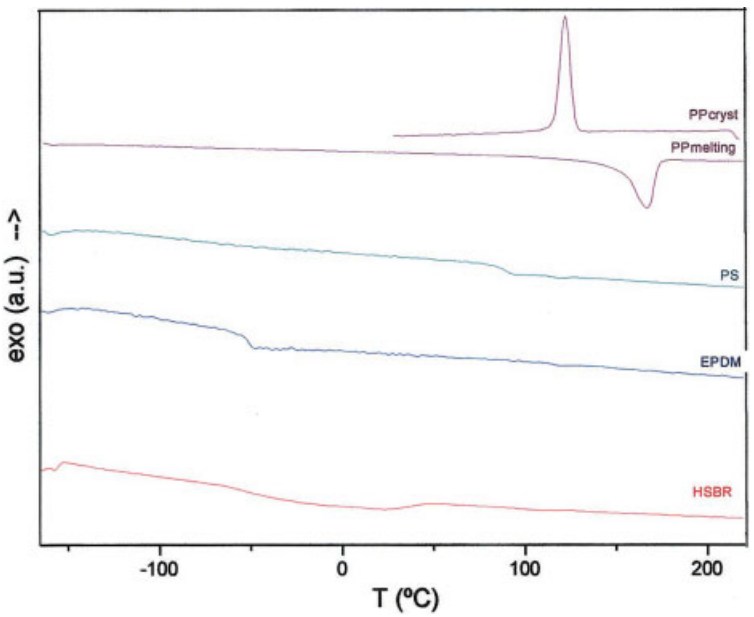

Figure 1 Thermograms of the initial materials.

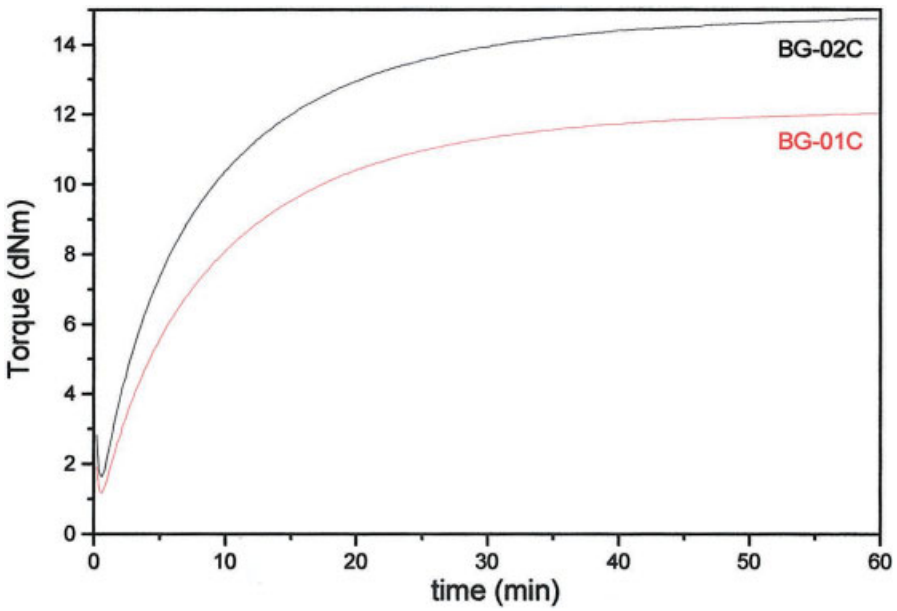

Figure 2 Rheograms of the HSBR/EPDM/PP blends.

nated blends. Figure 1 shows the thermograms of the initial materials. Sulfonation of the polymeric films causes T_g to rise significantly, as a consequence of the random incorporation of —SO_3H units all along the polymeric backbone. This triggers substantial changes in the physical properties of these materials, as a consequence of the emergence of ionic associations (clusters, multiplets, etc.), which reduce backbone mobility.[7]

The heterogeneous sulfonation reaction was achieved by placing the films in chlorosulfonic acid dissolved in 0.2*M* DCE for 4–6 h, depending on blend type. After sulfonation, the samples were washed in methanol and then in water.

RESULTS

The HSBR/EPDM/PP system

The curing rheograms of the blends prepared according to the method described in the experimental part of this work are reproduced in Figure 2, plotting torque against time, for the two blends with different PP portions. The rheograms allow us to determine the most suitable process time [i.e., at the point where 97% transformation is reached (t_{97}), which in our case is 37–38 min]. The shape of the graphs, which is similar for both samples, suggests two chemically very stable blends. So, the degradation problem can be discarded. The processes are fairly speedy, as can be seen from the steep ascending part of the graph, which then, for instance, when the curing optimum is reached, presents a large plateau—the horizontal part, during which there is no variation in material properties.

The peroxide curing mechanism occurs, for these systems, according to a radical-like process of polymerization.[8]

For the purpose of determining their mechanical properties, the noncrosslinked and cured samples were subjected to several mechanical tests. Table II compiles the different test results. The values obtained show, in general, all the mechanical properties notably to improve with curing. Prior to curing, hardly any properties are appreciated in the blends. It is worth highlighting that tensile strength is considerably lower. In contrast, hardness value variation is rela-

TABLE II
Results Obtained from the Traction Properties, Residual Strain, and Hardness Tests of These Samples with PP

Property	BG-01	BG-01C	BG-01Cslf	BG-02	BG-02C	BG-02Cslf
Stress at 100% (MPa)	—	4.07	—	2.88	5.30	—
Stress at 300% (MPa)	—	10.85	—	—	—	—
Tensile stress (MPa)	3.94	8.49	14.54	2.74	8.64	15.45
Elongation at break (%)	77	222	44.2	157	180	85.9
Microhardness	71.0	66.0	83.0	63.0	67.0	92.0
Residual strain (%)	—	26	—	—	29	—

TABLE III
Major Thermal Transitions of the PP Blends

Sample	T_g (°C)	T_m (°C)	T_c (°C)
BG-01	−53.05	162.48	—
BG-01C	−53.85	160.98	—
BG-01Cslf	−36.50	160.25	—
BG-02	−55.23	164.01	109.89
BG-02C	−53.51	161.56	110.72
BG-02Cslf	−30.41	161.85	108.58
HSBR	−56.12	—	—
EPDM	−51.48	—	—
PP	—	164.97	123.13

tively low, yet it increases remarkably with sulfonation. The same applies to tensile strength. Nevertheless, once sulfonated, the samples present less elongation at break.

Finally, the samples were microstructurally analyzed by DSC. Table III shows the values of the transitions recorded for the noncrosslinked, cured, and sulfonated samples, as well as for the unblended materials, indicating the values of the glass transitions, melting temperature (T_m), and crystallization temperature (T) of PP. Figure 3 shows the respective thermograms. No significant differences in the thermal transitions are observed before and after curing, but they do appear as a result of sulfonation. Between −53 and −55°C, there appears a clear transition, which is the T_g zone of the butadiene in HSBR, as well as that of EPDM, probably with some overlap. After sulfonation, this same transition appears at a higher temperature (i.e., between −30 and −35°C due to cluster formation, as was already stated). In addition, a minor exothermal transition is observed around 45°C (Fig. 4, thermograms 2′ and 3′), most likely due to internal rearrangement of the crystalline units, as a consequence of ion clustering.

In the heating scan, there appears an endothermal transition in the range between 160 and 164°C (thermograms 1, 2, 3, and 4), indicative of the PP melting process. The cooling scan shows an exothermal transition (thermograms 1′, 2′, 3′, and 4′) around 110°C, which corresponds to PP crystallization, but is only observed for the blends with a major crystalline PP portion.

The HSBR/EPDM/PS system

The crosslinking process of these systems follows the same reaction scheme as described in the previous chapter. Figure 5 shows the curing graphs as obtained from plotting torque against time. The t_{97} values for the two compositions with PS also present after some 37 min. In addition, the similar shape of the graph with a steep part followed by a wide plateau is indicative of the fact that, similar to the previously discussed PP systems, we are in the presence of stable blends and fast curing processes.

Table IV compiles the results obtained from the traction properties, residual strain, and hardness tests of these samples. Prior to curing, the mechanical properties are on the whole fairly poor. Tensile strength is the property which undergoes the greatest variation as a consequence of both crosslinking and sulfonation. It is worth emphasizing that sulfonation also reduces elongation at break. Hardness likewise varies considerably: it increases notably after crosslinking and sulfonating the blends.

DSC yields the thermograms represented in Figures 6 and 7, before and after curing and sulfonation, respectively. The transitions are compiled in Table V.

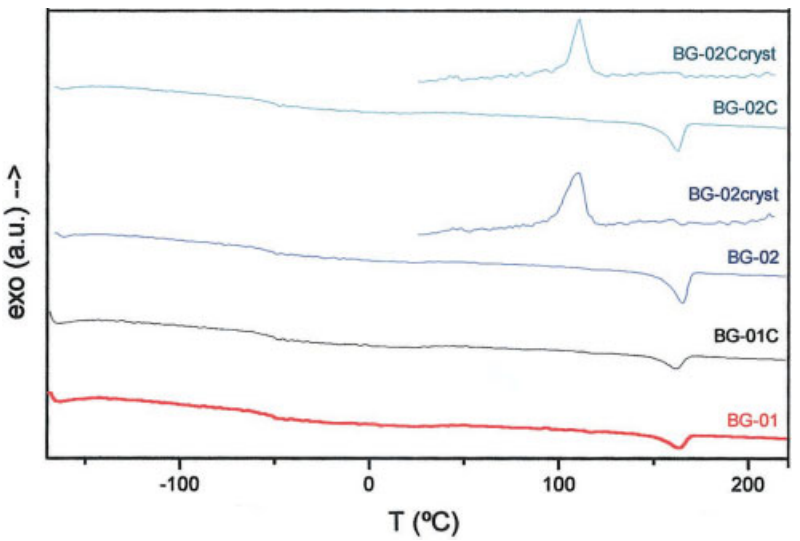

Figure 3 Thermograms of the noncrosslinked and cured samples.

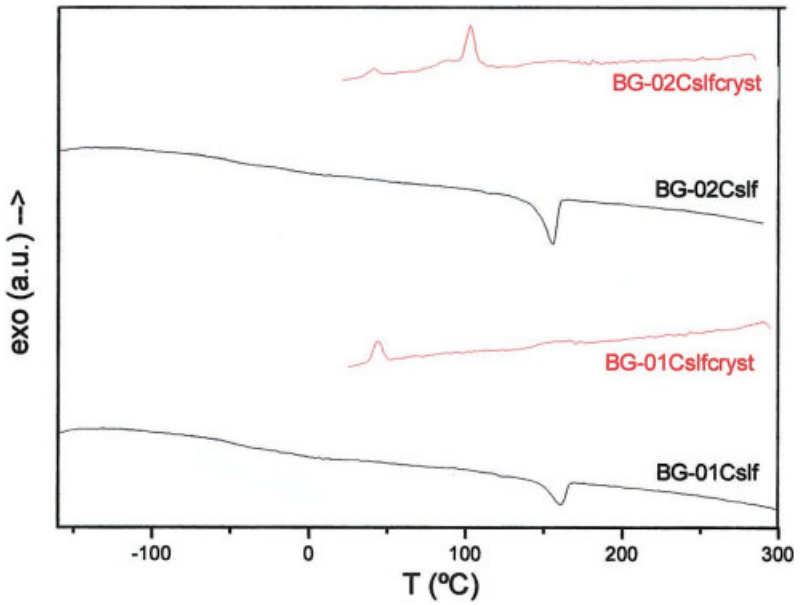

Figure 4 Thermograms of the sulfonated samples.

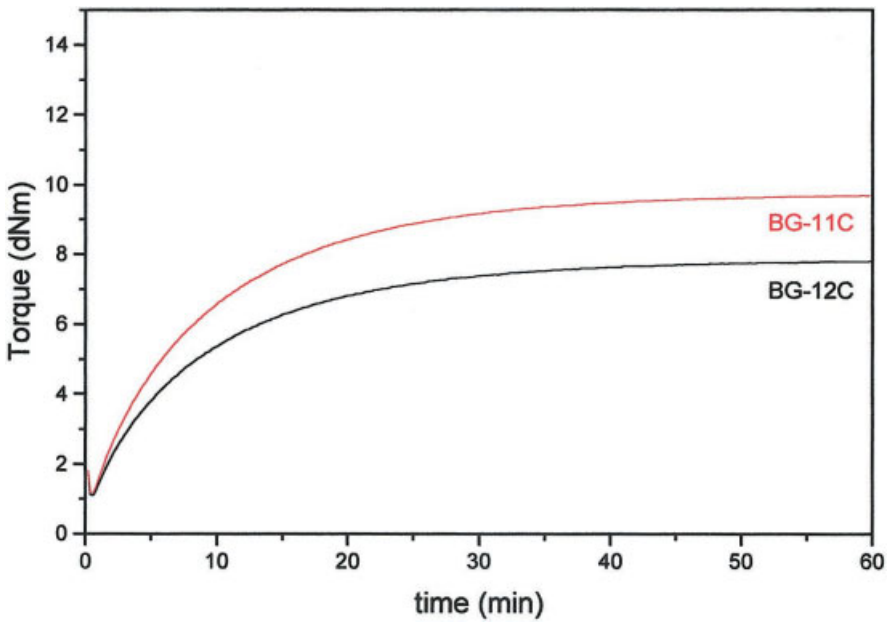

Figure 5 Rheograms of the HSBR/EPDM/PS blends.

TABLE IV
Results Obtained from the Traction Properties, Residual Strain, and Hardness Tests of These Samples with PS

Property	BG-11	BG-11C	BG-11Cslf	BG-12	BG-12C	BG-12Cslf
Stress at 100% (MPa)	1.46	3.91	—	2.05	6.21	—
Stress at 300% (MPa)	—	—	—	—	—	—
Tensile stress (Mpa)	1.76	7.60	14.92	2.10	10.81	13.83
Elongation at break (%)	149	151	56.9	120	184	99.0
Microhardness	43.0	58.5	78	45.5	54.0	85
Residual strain (%)	—	33	—	—	47	—

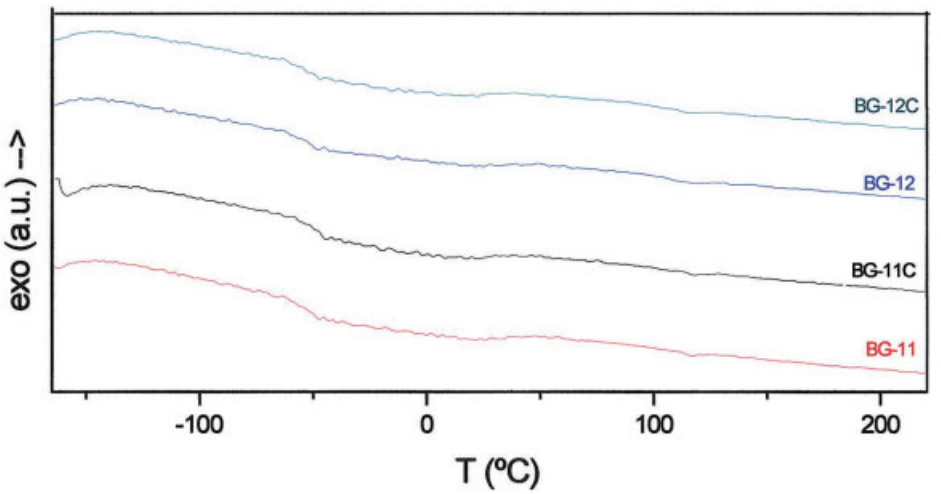

Figure 6 Thermograms of the noncrosslinked and cured samples.

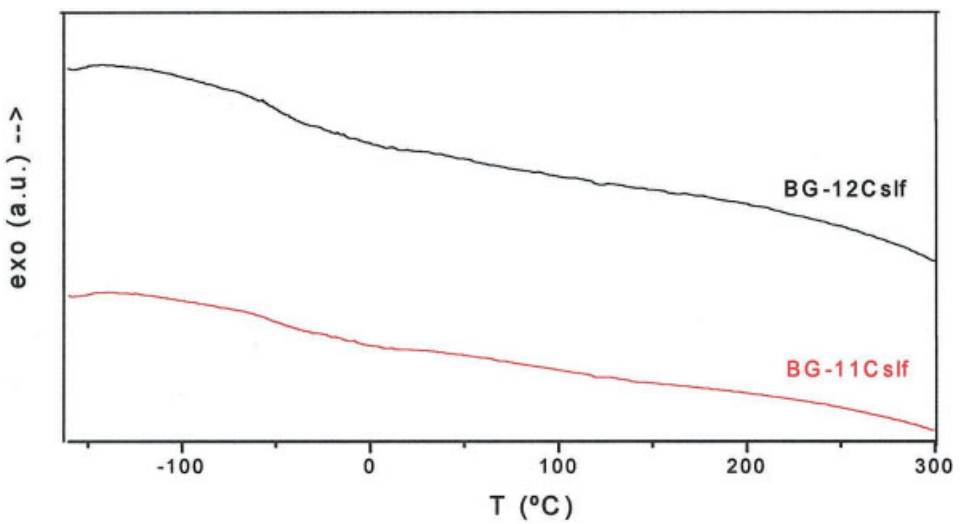

Figure 7 Thermograms of the sulfonated samples.

For these blends, a single transition is observed, T_g, also around −54°C, without any appreciable change after curing. Yet it is shifted to higher temperatures upon sulfonation, to approximately −35°C, due to ion-clustering. However, no separate polystyrene T_g is observed.

The HSBR/EPDM/silica system

The crosslinking reaction undergone by these materials is also a radical-like process, analogous to the one described above. Figure 8 shows the rheograms obtained in the course of the curing study. The t_{97} values calculated from the graphs are slightly lower for the two silica-containing blends than for the other two systems discussed in the two previous chapters, presenting at 23 and 28 min, respectively, depending on the greater or lesser silica component in the blend. Similar to the other two systems, these blends are very stable. Hence, there is no material degradation risk in increasing the curing time by a few minutes, thus ensuring process optimization.

TABLE V
Major Thermal Transitions of the PS Blends

Sample	T_g (°C)
BG-11	−54.18
BG-11C	−53.84
BG-11Cslf	−35.54
BG-12	−54.04
BG-12C	−54.10
BG-12Cslf	−36.50
HSBR	−56.12
EPDM	−51.48
PS	88.52

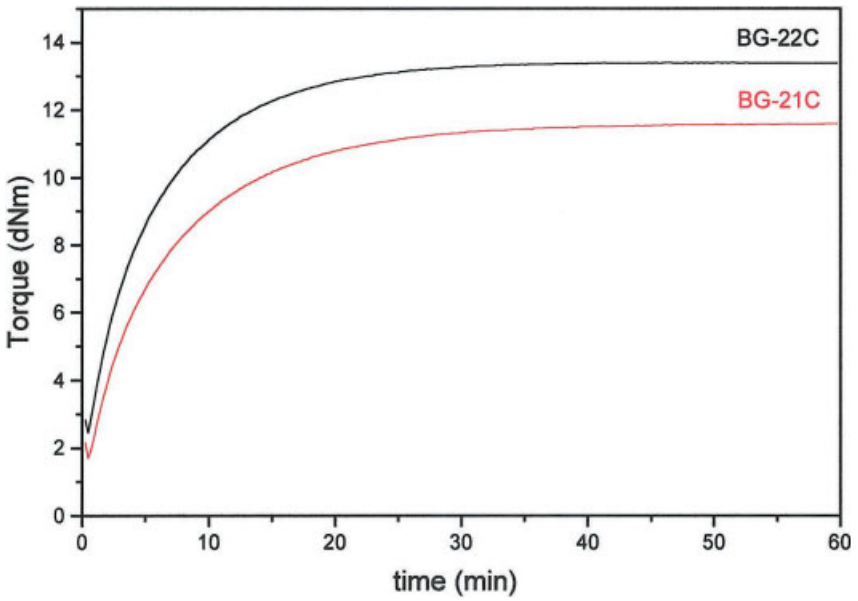

Figure 8 Rheograms of the HSBR/EPDM/silica blends.

TABLE VI
Results Obtained from the Traction Properties, Residual Strain, and Hardness Tests of These Samples with Silica

Property	BG-21	BG-21C	BG-21Cslf	BG-22	BG-22C	BG-22Cslf
Stress at 100% (MPa)	—	3.77	—	—	4.26	—
Stress at 300% (MPa)	—	—	—	—	—	—
Tensile stress (MPa)	1.89	6.04	11.85	1.74	8.13	15.17
Elongation at break (%)	85.5	197	24.6	96.6	229.8	38.8
Microhardness	49.0	64.0	80.0	55.0	66.0	83.0
Residual strain (%)	—	46	—	—	43	—

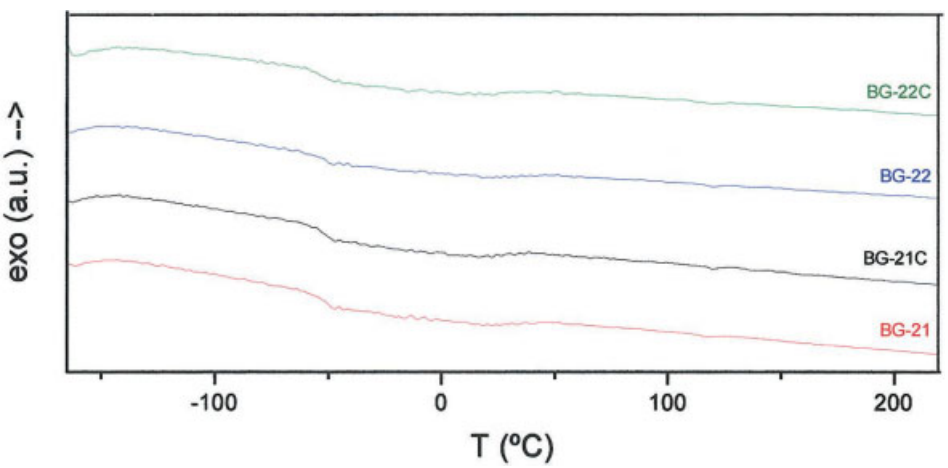

Figure 9 Thermograms of the noncrosslinked and cured samples.

As regards the mechanical properties of these silica blends, the traction properties, residual strain, and hardness test data are indicated in Table VI. All mechanical properties improve considerably with curing. Tensile strength is greatly enhanced with sulfonation, and elongation at break shows an identical reduction with sulfonation, as observed for the other two systems. Hardness improves as a consequence of both curing and sulfonation.

Figures 9 and 10 show the DSC thermograms for the untreated, cured, and finally, sulfonated samples. Table VII compiles the transition values recorded. Similar to what was stated for the other two systems, the silica-containing samples show the same T_g in the

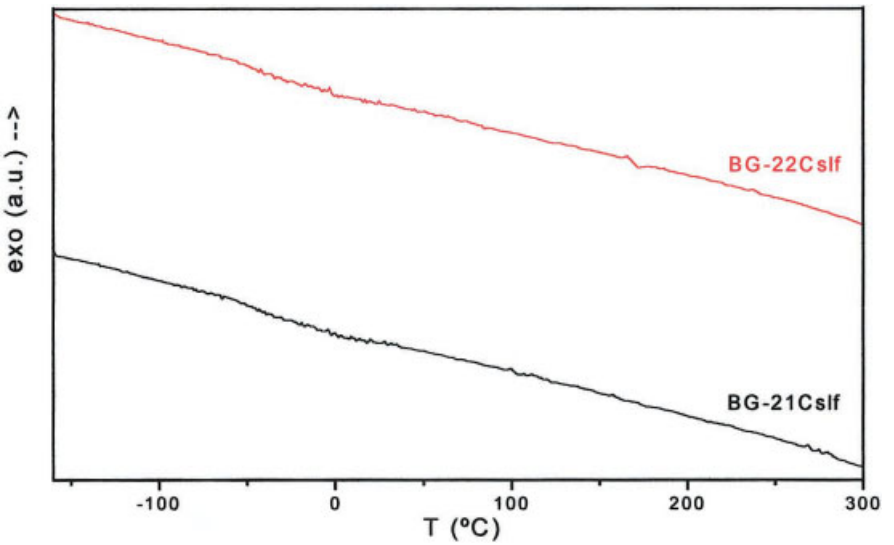

Figure 10 Thermograms of the sulfonated samples.

TABLE VII
Major Thermal Transitions of the Silica Blends

Sample	T_g (°C)
BG-21	−53.99
BG-21C	−53.18
BG-21Cslf	−42.39
BG-22	−54.68
BG-22C	−53.66
BG-22Cslf	−35.23
HSBR	−56.12
EPDM	−51.48

initial temperature range around −54°C and a shift to higher temperatures, between −40 and −35°C, consequential to ion-cluster formation upon sulfonation.

CONCLUSION

In light of the results obtained, it is legitimate to state that in all cases we have been dealing with stable materials from a thermal and chemical point of view, free of any degradation bias, which, once cured, all present with reinforced mechanical properties.

The systems containing a PP component show the greatest mechanical strength and the smallest residual strain percentile, as they possess a crystalline portion in their structure. Yet the other systems show a similar hardness.

Comparison of the principal properties analyzed for the different systems yields the following results.

Figure 11 shows the microhardness data as a function of a PP, PS, or silica component in the blends. The greatest hardness is achieved for the sulfonated systems [Fig. 11(C)]. No significant change in this value is observed because of a major or lesser PP, PS, or silica component content in the blends.

The samples showing the highest hardness values all have a PP component. The PS blends, in contrast, have the lowest hardness values, both prior to and

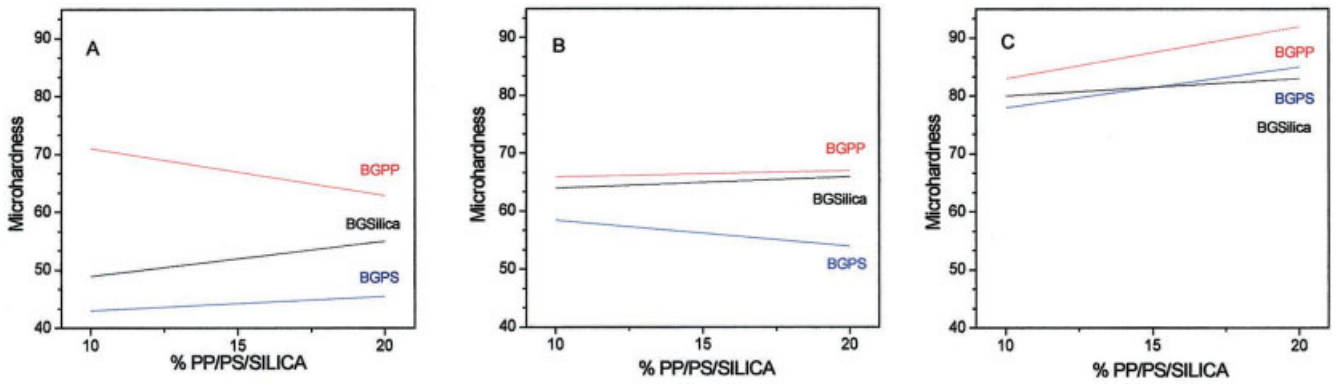

Figure 11 Microhardness data as a function of a PP, PS, or silica content in the blend. (A) Noncrosslinked samples; (B) cured samples; (C) sulfonated samples.

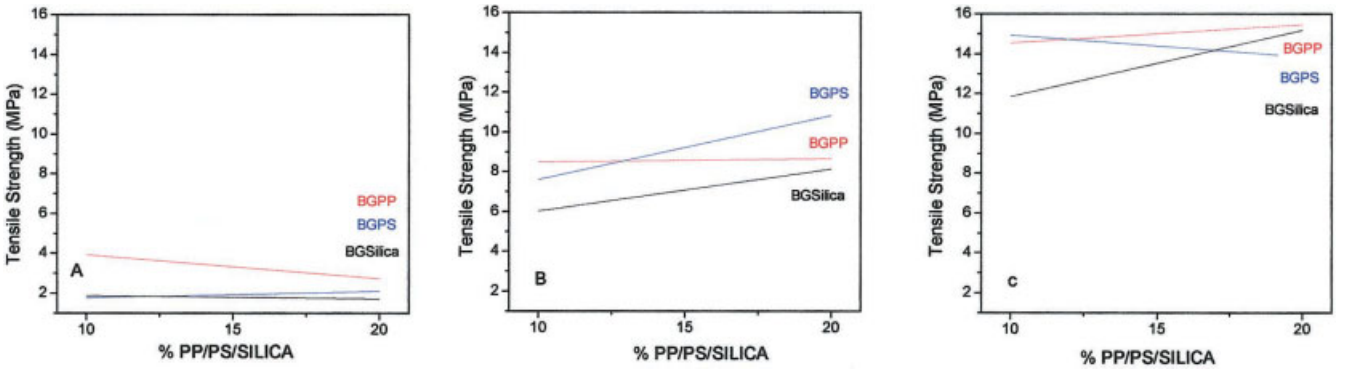

Figure 12 Tensile strength as a function of a PP, PS, or silica content in the blend. (A) Noncrosslinked samples; (B) cured samples; (C) sulfonated samples.

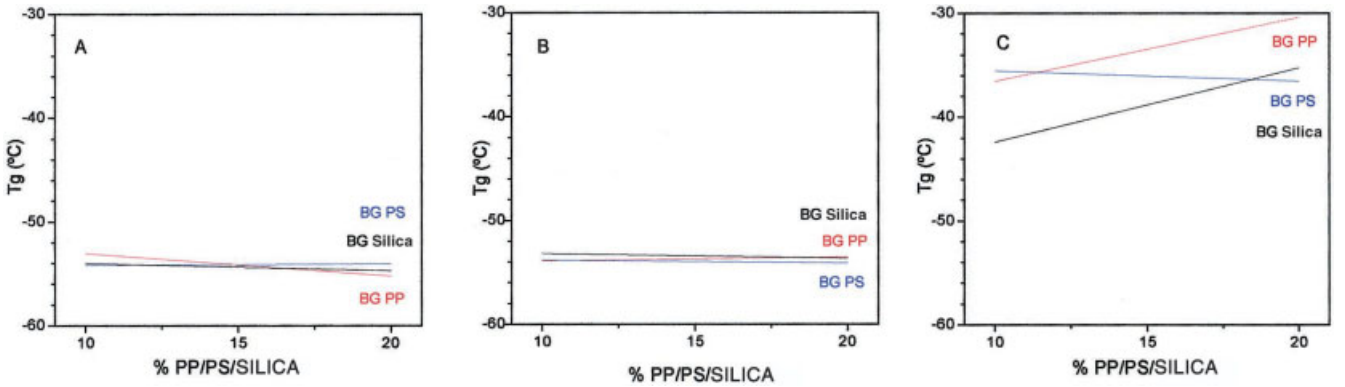

Figure 13 Glass transition temperature as a function of a PP, PS, or silica content in the blend. (A) Noncrosslinked samples; (B) cured samples; (C) sulfonated samples.

after crosslinking. Once sulfonated, their hardness values approach those of the silica blends.

Figure 12 shows tensile strength plotted against composition. This property presents low values for all blends prior to crosslinking, although the PP samples have slightly higher values. After curing, these values rise, which also applies to the effect of sulfonation.

Break strength proves to have little sensitivity regarding the third component in the blend, be it PP, PS, or silica, although there are some cases where the value rises, such as the crosslinked PS and silica samples [Fig. 12(B)] and the sulfonated silica sample [Fig. 12(C)].

Figure 13 shows the glass transition temperature of all the blends, as a function of PP, PS, or silica content. In no case, significant differences are observed in the T_g values before and after curing [Fig. 13(A, B)]. After sulfonation [Fig. 13(C)], however, T_g presents a significant rise because of the appearance of clusters, as was already commented on, due to the incorporation of —SO_3H units into the polymeric backbone.

References

1. Sossina, M. Haile Acta Mater 2003, 51, 5981.
2. Carrette, L. K.; Friedrich, A.; Stimming, U. Fuel Cells 2001, 1, 5.
3. Prater, K. B. J. Power Sources 1996, 61, 105.
4. Strasser, K. J. Power Sources 1992, 37, 209.
5. Carrette, L. K.; Friedrich, A.; Stimming, U. Chem Phys Chem 2000, 1, 162.
6. Royo, J. Manual de Tecnología del Caucho Ed Consorcio Nacional de industriales del caucho, 2nd ed.; Reclamo Técnico: Barcelona.
7. Eisemberg, A. Macromolecules 1970, 3, 147.
8. Brydson, J. A. Rubber Chemistry; Applied Science Publishers: London, 1978.